ACS APPLIED MATERIALS & INTERFACES

Research Article

www.acsami.org

Molecular Structure Effect of Pyridine-Based Surface Ligand on the Performance of P3HT:TiO_2 Hybrid Solar Cell

Jhih-Fong Lin,[†] Guang-Yao Tu,[‡] Chun-Chih Ho,[†,§] Chun-Yu Chang,[†] Wei-Che Yen,[‡] Sheng-Hao Hsu,[‡] Yang-Fang Chen,[⊥] and Wei-Fang Su*[,†,‡]

[†]Department of Materials Science and Engineering, [‡]Institute of Polymer Science and Engineering, [§]Graduate Institute of Photonics and Optoelectronics, and [⊥]Department of Physics, National Taiwan University, No. 1, Sec. 4, Roosevelt Road, Taipei, 10617 Taiwan

Supporting Information

ABSTRACT: Colloid TiO_2 nanorods are used for solution-processable poly(3-hexyl thiophene): TiO_2 hybrid solar cell. The nanorods were covered by insulating ligand of oleic acid (OA) after sol-gel synthesis. Three more conducting pyridine type ligands: pyridine, 2,6-lutidine (Lut) and 4-tert-butylpyridine (tBP) were investigated respectively to replace OA. The power conversion efficiency (PCE) of the solar cell was increased because the electronic mobility of pyridine-type ligand-modified TiO_2 is higher than that of TiO_2−OA. The enhancement of PCE is in the descending order of Lut > pyridine > tBP because of the effective replacement of OA by Lut. The PCE of solar cell can be further enhanced by ligand exchange of pyridine type ligand with conjugating molecule of 2-cyano-3-(5-(7-(thiophen-2-yl)-benzothiadiazol-4-yl) thiophen-2-yl) acrylic acid (W4) on TiO_2 nanorods because W4 has aligned bandgap with P3HT and TiO_2 to facilitate charge separation and transport. The electronic mobility of two-stage ligand exchanged TiO_2 is improved furthermore except Lut, because it adheres well and difficult to be replaced by W4. The amount of W4 on TiO_2-tBP is 3 times more than that of TiO_2−Lut (0.20 mol % vs. 0.06 mol %). Thus, the increased extent of PCE of solar cell is in the decreasing order of tBP > pyridine > Lut. The TiO_2-tBP-W4 device has the best performance with 1.4 and 2.6 times more than TiO_2-pyridine-W4 and TiO_2-Lut-W4 devices, respectively. The pKa of the pyridine derivatives plays the major role to determine the ease of ligand exchange on TiO_2 which is the key factor mandating the PCE of P3HT:TiO_2 hybrid solar cell. The results of this study provide new insights of the significance of acid-base reaction on the TiO_2 surface for TiO_2-based solar cells. The obtained knowledge can be extended to other hybrid solar cell systems.

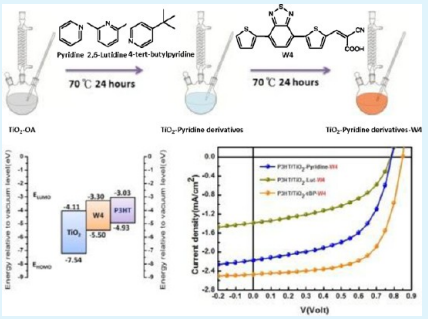

KEYWORDS: *polymer, nanoparticle, surface modifier, ligand exchange, hybrid solar cell, power conversion efficiency*

INTRODUCTION

In recent years, organic photovoltaics (OPV) have drawn much attention because of their low cost of processing, light weight, flexibility, and ease of large-sized fabrication. In general, the bulk heterojunction (BHJ) structure of OPV is the most effective way to achieve high power conversion efficiency. The BHJ is composed of conjugating polymer as donor and nanoparticles as acceptor. The fullerene derivative [6,6]-phenyl-C61-butyric acid methyl ester ($PC_{61}BM$) is commonly used as acceptor for its good compatibility with conjugating polymers. To improve the power conversion efficiency, many research groups have synthesized various conjugating polymers to increase light harvesting and improve charge injection.[1−4] Meanwhile, to have better morphological control in BHJ solar cell, $PC_{71}BM$ and other fullerene derivatives are used in OPV devices.[5−7] However, the fullerene derivatives in bulk heterojunction are easily aggregated under heat thus degrade the devices performance. The poor thermal stability of polymer:fullerene system is still an obstacle for the commercialization of OPV. To avoid the thermal aggregation of fullerene derivatives in BHJ solar cell, the fullerene derivatives can be replaced by more thermal stable inorganic nanocrystals in bulk heterojunction structure to make hybrid solar cell.[8] There are various nanocrystals that have been used in OPV devices such as CdS,[9] PbS,[10] CdTe,[11] CdSe,[12−14] ZnO,[15−19] and TiO_2.[20−23] The advantages of incorporating nanocrystals into organic BHJ solar cell including good thermal stability, better carrier mobility, controllable size, and tunable band structure. However, according to the above studies, the main problems of polymer:nanocrystals hybrid solar cell are the insulating ligands and defects on the surface of nanocrystals. In addition, the compatibility between polymer and nanocrystals also induces severe phase separation and reduces the performance of devices.

Poly(3-hexyl thiophene): TiO_2 system (P3HT:TiO_2) has shown its potential in OPV application for good thermal stability and durability.[20−25] To solve the problem of low power conversion efficiency in P3HT:TiO_2 hybrid solar cell, we took two-stage surface modification on TiO_2 nanorods and study the mechanism of ligand exchange. According to our previous work,[23] the insulating oleic acid attached on TiO_2 surface was partially replaced by pyridine in the first-stage of surface

Received: November 14, 2012
Accepted: January 16, 2013
Published: January 16, 2013

   dx.doi.org/10.1021/am302700c | *ACS Appl. Mater. Interfaces* 2013, 5, 1009−1016

modification.Then, in the second-stage of surface modification, we introduced band aligned surface modifier such as oligomer-3-hexylthiophene and commercial dyes onto the surface of TiO_2 nanorods. As the bridge of charge transport between conducting polymer P3HT and TiO_2 nanorods, the surface modifier could facilitate the charge separation and transport between P3HT and TiO_2 nanorods. However, the mechanism of ligand exchange process is still unclear, especially in the quantitative aspect. In this study, we carry out the systematic study of molecular structure effects of pyridine type ligands on the device performance of P3HT: TiO_2 hybrid solar cell by carefully analyzing the amount of ligand on the TiO_2 surface and deduced the mechanism of ligand exchange.

RESULTS AND DISCUSSION

According to our previous studies,[20−22] we found the surface modifier such as pyridine and other conjugating surface modifier could repair the surface defects of TiO_2 in modification process and enhance the performance of P3HT: TiO_2 hybrid solar cell. On the other hand, to evaluate the effect of pyridine and other conjugating surface modifier in surface modification process, we adapt a two-stage surface modification rather than single-stage surface modification (see the Supporting Information, Figure S1 and Table S1) on TiO_2 as shown in Figure 1a. In the first-stage of surface modification, we

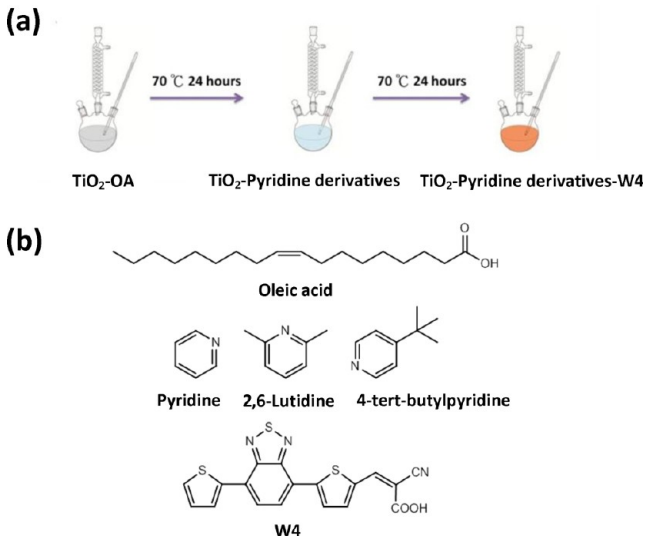

Figure 1. (a) Schematic diagram of two-stage surface modification for TiO_2. (b) Molecular structures of oleic acid and pyridine derivatives.

applied three different pyridine type ligands (pyridine, 2,6-Lutidine (Lut), and 4-tert-butylpyridine (tBP)), respectively, on TiO_2, their chemical structures are shown in Figure 1b and their properties are summarized in Table 1. Comparing the molecular structure of OA with the pyridine derivatives, the delocalization of π electrons from pyridine derivatives is more conducting than the long alkyl chain from OA. Such replacement of conducting pyridine derivatives could avoid the charge trapping and recombination on the surface of TiO_2. In addition, we speculate that the pyridine derivative attached on TiO_2 would assist the attachment of conjugating surface modifier on TiO_2 on the second stage of replacement, because the effective frequency factor of ligand exchange reaction is increased due to the increasing compatibility between two components. Therefore, controlling the two-stage interface

Table 1. Properties of Oleic Acid and Three Different Pyridine-Type Ligands

property	oleic acid	pyridine	2, 6-lutidine	4-tertbutyl-pyridine
molecular formula	$C_{18}H_{34}O_2$	C_5H_5N	C_7H_9N	$C_9H_{13}N$
boiling temperature (°C)	360	115.2	144	196
surface tension (dyne:cm)[40,41]	32.8	38.0	33.2	29.9
dipole moment (Debye)[a]	1.55	2.38	1.56	3.03
pK_a[42]		5.2	6.7	6.0

[a]The dipole moment was calculated from the mechanical package Gaussian 03.

engineering to obtain the highest coverage of conjugating surface modifier on TiO_2 is imperative to facilitate the charge transport and further improve device performance of P3HT: TiO_2 hybrid solar cell.

The pyridine derivatives are not only the surface modifier but also play the role of solvent in the first-stage of surface modification of TiO_2 nanorods, so we need to add excess hexane to precipitate out the modified TiO_2 and remove the residual solvent before the characterization of ligand compositions on TiO_2 surface. The weight percentage of carbon (C), nitrogen (N), and hydrogen (H) of different pyridine-derivative-modified TiO_2 samples was determined by elemental analysis. The results are summarized in Table 2. Taking the molecular formula of different ligands into account, we converted the weight percentage of carbon (C), nitrogen (N), and hydrogen (H) to molar percentage of oleic acid and pyridine derivative molecules. It is noteworthy that the remained nitrogen in TiO_2−OA sample may come from the remaining catalyst trimethylamine-N-oxide dihydrate (TMAO) in sol-gel process. Thus, we subtracted this value for all of the samples to avoid any analysis error. In the first-stage of surface modification, there were a large number of collisions happened between the TiO_2−OA and pyridine derivatives during the replacement reaction. For an effective collision, the lone pair electron of pyridine derivatives should occupy the empty orbital of Ti atoms and induce desorption of OA from TiO_2 surface. It is interesting to note that the coverage of surface modifiers on TiO_2 is different among three pyridine derivatives after the calculation of the amount of ligands remained and overall available Ti positions on the surface of TiO_2 nanorod. The Lut attached on TiO_2 exhibited the highest coverage (45.7%). On the other hand, tBP removed OA most efficiently but it had the lowest coverage (28.3%) on TiO_2. The pyridine derivatives may attach to Ti atom at 5-folded-coordinated position through its lone pair electrons. It is like a reaction of Lewis acid and base. The lone pair electrons of pyridine derivatives shows especially high reactivity toward Ti^{3+} defects. The reactivity is also dependent on the pKa of pyridine derivative as listed in Table 1. The larger pKa value represents the higher density of lone pair electron. Thus, the amount of pyridine derivatives on TiO_2 after the first-stage modification is in the descending order of Lut > tBP > pyridine, in according with their pka value. To make sure the presence of ligand on TiO_2 surface, we employed X-ray photoelectron spectroscopy (XPS) to collect the nitrogen information on pyridine derivative modified TiO_2 nanorods. As shown in Figure 2, we can find the trace of nitrogen in TiO_2−Lut and TiO_2−tBP, but it is not obvious in TiO_2−pyridine sample. The highest intensity of N_{1s} electron in TiO_2−Lut

Table 2. Weight and Molar Percentage of Surface Ligands on TiO_2 nanorods

				no. of surface ligands per TiO_2 nanorod		coverage of surface ligands on TiO_2 nanorod (%)[b]	
sample	N (wt %)	C (wt %)	H (wt %)	pyridine derivative	OA	pyridine derivative	OA
TiO_2–OA	0.18[a]	20.20	3.67	0	1817	0	61.6
TiO_2–Pyridine	0.39	14.66	3.19	276	1147	9.4	38.9
TiO_2–Lut	1.17	18.17	3.50	1347	1069	45.7	36.6
TiO_2–tBP	0.63	13.41	3.07	432	834	14.7	28.3

[a]The trace of nitrogen was from the remaining catalyst trimethylamine-N-oxide dihydrate (TMAO) in TiO_2 hydrolysis process. The same value of nitrogen was subtracted for all the samples to avoid the analysis error. [b]The coverage of surface lingands on TiO_2 is calculated by the ligand occupied on Ti atom at 5-fold-coordinated position of TiO_2 nanorods surface.

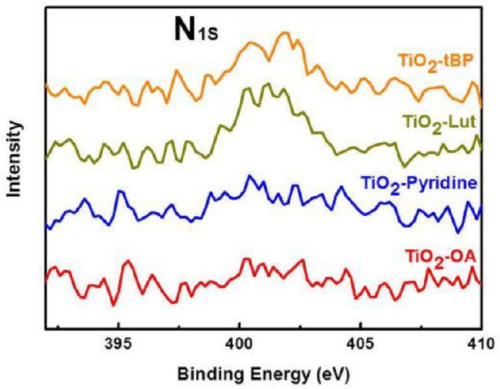

Figure 2. X-ray photoelectron spectra of nitrogen for TiO_2 modified by different ligands.

observed among the samples is consistent with the results of elemental analysis.

In our previous study,[23] we assumed the ligand exchange of inorganic nanocrystal was completed after each stage by sequentially removal of remaining ligands and attaching of new surface modifiers at 70°C. It is interesting to note that the amount of OA removing and pyridine derivatives attaching are all different depending on the type of pyridine as shown in Table 2. The removing amount of OA is in the descent order of tBP>Lut>Pyridine but the OA was not completely replaced by any of the pyridine derivatives after the first stage of ligand exchange. The lowest surface tension of tBP is the most compatible with OA, which can replace the OA most effectively, so the least amount of OA remained on the TiO_2. The pyridine has the highest surface tension and cannot replace OA as effective as Lut and tBP, which results in the highest amount of OA remained on TiO_2. Apparently, the mechanism of replacing OA by pyridine type ligand involves removing OA and attaching the pyridine derivative on TiO_2. The OA is known to be attached on TiO_2 by chelating the carboxylic group of OA onto TiO_2 to form coordination bond.[30] Under the ligand exchange reaction, the reactant of pyridine type ligand is a solvent and in excess amount which can constantly collide with TiO_2–OA in a large extent, the driving force between the Lewis base of pyridine derivative and acid of TiO_2 is likely to replace the bonding between TiO_2 and OA. That results in the replacement of OA by pyridine type ligand on TiO_2. The ease of replacement depends on many parameters such as reaction temperature and time, the bonding strength between ligand and TiO_2, the polarity, solubility, dipole moment, pKa, etc. of replacing and being replaced ligands. A detailed study of the rate of replacement reactions that involves carrying out the reaction at different temperature and identifying the reaction products will be reported in the future.

According to the operation principle of BHJ polymer solar cell such as P3HT:TiO_2 hybrid solar cell, P3HT absorbs solar light to generate excitons, the excitons must diffuse to the interface of hybrid and be separated by the internal electric field between of P3HT and TiO_2. However, the insulating OA molecule covered on TiO_2 surface causes many charges to be recombined, because the separated charges cannot transport through the insulating OA directly rather by hopping. After the first-stage of surface modification, the OA was replaced by more conducting pyridine derivative, an improved charge transport should be expected. To determine the electron mobility of TiO_2 modified by different ligands, we selected appropriate Al electrode for the diode and employed space charge limited current (SCLC) model (eq 1). The results are plotted and shown in panels b and c in Figure 3. According to eq 1, ε is equal to $\varepsilon_r\varepsilon_0$. For TiO_2, the relative permittivity ε_r is about 50, V_{eff} is effective potential drop inside the active materials. μ and L are carrier mobility and film thickness respectively.

$$J = \frac{9}{8}\varepsilon\mu\frac{V_{eff}^2}{L^3} \quad (1)$$

After the first stage of surface modification with different pyridine derivatives respectively on TiO_2, the electronic mobility of TiO_2 is enhanced in accordance of the removing amount of OA from TiO_2 surface. In TiO_2–tBP thin film, the least amount of OA molecules was on the TiO_2 surface, and its electron mobility was improved by close to two orders (from 2.93×10^{-6} $cm^2/(V\ s)$ to 4.69×10^{-4} $cm^2/(V\ s)$) than that of TiO_2–OA. But, the OA is the best dispersion aid that helps the TiO_2 nanorods to be dispersed into the polymer domain. Hence, after blending with P3HT, the electron mobility of P3HT: TiO_2–tBP thin film decreases dramatically (8.70×10^{-7} $cm^2/V{\cdot}s$) as shown in Figure 3c. It is lower than that of P3HT: TiO_2–Pyridine (2.10×10^{-7} $cm^2/V{\cdot}s$) and P3HT: TiO_2–Lut (1.70×10^{-7} $cm^2/(V\ s)$). To clarify this phenomenon, we used transmission electron microscopy to investigate the distribution of TiO_2 nanorods in different P3HT:TiO_2 hybrid films. Figure 4 shows the dispersion of the 2,6-lutidine modified TiO_2 in P3HT was the best among all the samples because the size of each domain is the smallest although TiO_2–Lut does not contain high amount of OA. That is due to the two methyl groups of 2,6-lutidine on TiO_2 helps dispersing well in P3HT. The TiO_2–tBP with least amount of OA has the worst dispersion in P3HT and also induces island-shaped aggregations. That explains the lowest electronic mobility of P3HT:TiO_2–tBP hybrid film. Furthermore, the isolated aggregation of TiO_2–tBP in P3HT matrix not only decreases

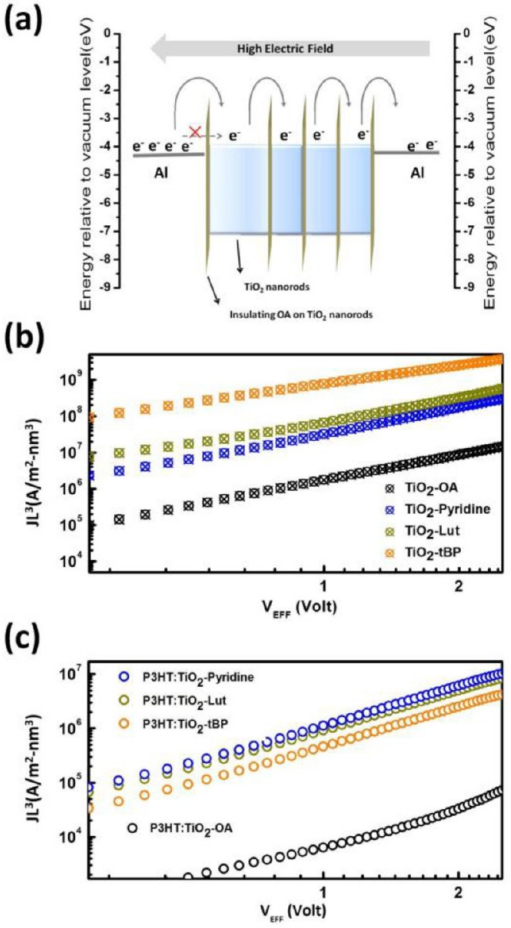

Figure 3. (a) Band structure of devices for SCLC measurement, the insulating ligand OA on TiO_2 surface is a barrier for electron transportation. Results of space charge limited current model from (b) TiO_2-(pyridine derivatives) thin film, (c) P3HT:TiO_2-(pyridine derivatives) thin film.

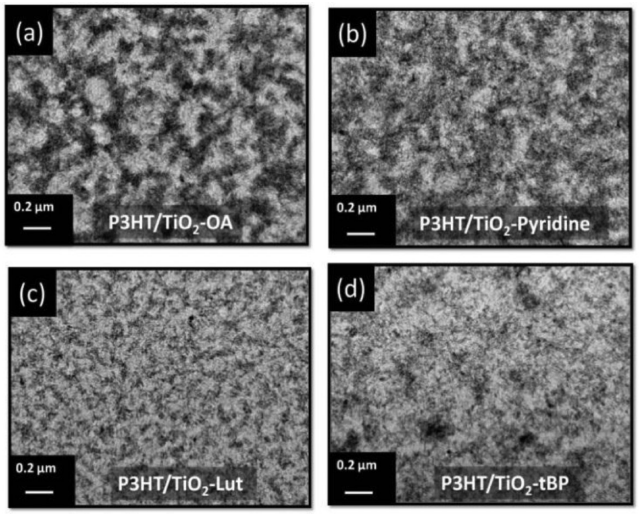

Figure 4. Transmission electron microscopy images of P3HT blends with (a) TiO_2−OA, (b) TiO_2−pyridine, (c) TiO_2−Lut, (d)TiO_2−tBP.

the amount of interface between P3HT and TiO_2 but limits the charge transport between isolated TiO_2 domains.

We studied the performance of P3HT:TiO_2 hybrid solar cells which were fabricated using TiO_2 modified by different pyridine derivatives. The results are shown in Figure 5 and Table 3. The TiO_2−Lut device has the highest short circuit

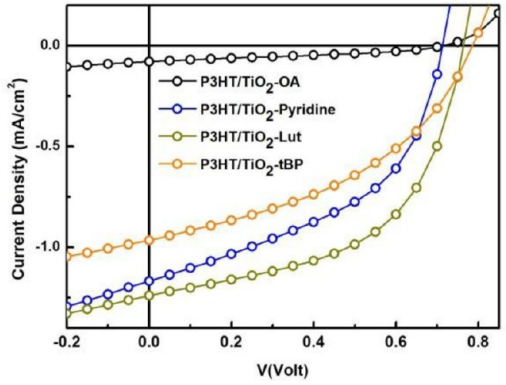

Figure 5. J−V curves of different P3HT:TiO_2−(pyridine derivative) devices.

current density (1.28 mA/cm^2) and the best device performance (0.51%) among three pyridine derivatives modified TiO_2 samples. Although the TiO_2-tBP has highest electron mobility, the low short circuit current density (0.97 mA/cm^2) and poor device performance (0.32%) show that the morphology of the hybrid film is a major factor to determine the performance of hybrid solar cell. The TiO_2−Pyridine does not have good dispersion in polymer matrix either, but it contains enough OA to form continuous percolation paths of TiO_2 in the hybrid thin film (Figure 4b) that reduces the extent of charge recombination, thus, shows a better solar cell performance than that of TiO_2-tBP. In addition, we also found that the TiO_2−Lut and TiO_2-tBP devices has higher open circuit voltage than TiO_2−Pyridine devices, the increasing of open circuit voltage has also seen in dye-sensitized solar cells.[31−36] This phenomenon is attributed from the decreased surface defects of TiO_2 from the attachment of Lut and tBP and reduced charge recombination.[37] Apart from this, the dipole moment of ligand also influences the interface building potential.[38,39] The larger dipole moment of attaching ligands would uplift the TiO_2 band structure and increase the effective bandgap between TiO_2 and P3HT (E_{C,TiO_2}−$E_{HOMO,P3HT}$). This also explains why tBP has highest open-circuit voltage in the device.

To further enhance the device performance of P3HT:TiO_2-pyridine derivative hybrid solar cell, we attached a conjugating molecule 2-cyano-3-(5-(7-(thiophen-2-yl)-benzothiadiazol-4-yl)thiophen-2-yl)acrylic acid (W4) (Figure 1b) on TiO_2. Via the second-stage of surface modification, the W4 was anchored on TiO_2 surface by carboxylic functional group at 70°C. In addition, the band alignment and conjugating π electrons of W4 molecules (Figure 6a) could facilitate the charge separation and transfer on TiO_2 and improve the device performance of P3HT: TiO_2 hybrid solar cell. To estimate the attached amount of W4 molecules on TiO_2 nanorods, we prepared a series of W4 solutions with known concentration and made a calibration curve from their absorption spectra. Subsequently, the TiO_2-pyridine derivative-W4 was washed and precipitated by hexane to remove unreacted W4 molecules. The TiO_2-pyridine derivative-W4 was then redispersed in pyridine. The solution was evaluated by UV-vis spectroscopy to determine the amount of remained W4 (Figure 6b). The TiO_2-tBP-W4 nanorods have highest amount of W4 molecules (0.62 mol %) attached on

Table 3. Photovoltaic Performance of Different P3HT:TiO_2 Devices

sample	μ_{e,TiO_2} ($\times10^{-5}$ $cm^2/(V\ s)$)	$\mu_{e,\ P3HT:TiO_2}$ ($\times10^{-7}$ $cm^2/(V\ s)$)	V_{OC} (V)	J_{SC} (mA/cm^2)	fill factor (%)	PCE (%)
P3HT:TiO_2−OA	0.29	0.024	0.72	0.08	34.94	0.02
P3HT:TiO_2−Pyridine	6	21	0.71	1.17	48.23	0.40
P3HT:TiO_2−Lut	12	17	0.76	1.28	53.37	0.51
P3HT:TiO_2−tBP	47	8.7	0.78	0.97	42.74	0.32
P3HT:TiO_2−Pyridine−W4	17	35	0.79	2.18	55.34	0.95
P3HT:TiO_2−Lut-W4	9	14	0.78	1.40	48.48	0.52
P3HT:TiO_2−tBP -W4	68	110	0.85	2.48	64.40	1.36

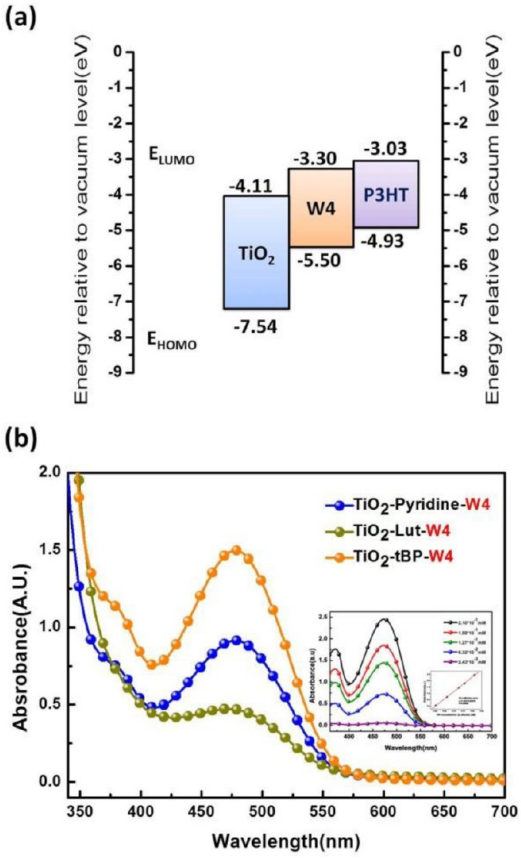

Figure 6. (a) Band alignment of W4 between P3HT and TiO_2 nanorods, and (b) the absorption spectra of different TiO_2−W4 solutions at the same concentration of TiO_2. The inset of (b) is the calibration curve of W4 solution with different concentrations determined by absorption spectroscopy.

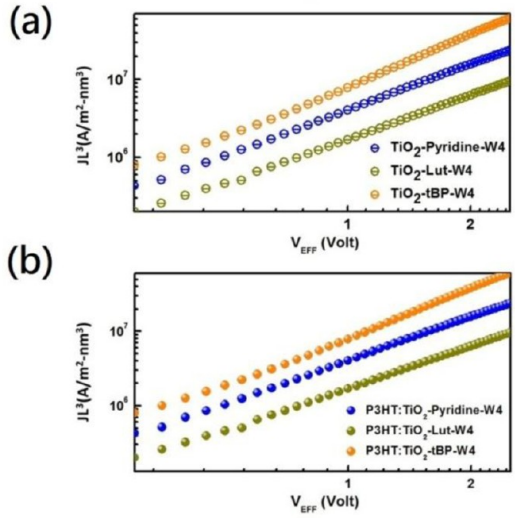

Figure 7. Electron mobility of different hybrid films determined by the space charge limited current model. (a) TiO_2−(pyridine derivatives)−W4 thin film, and (b) P3HT:TiO_2−(pyridine derivatives)−W4 hybrid thin film.

TiO_2 as compared to TiO_2−Pyridine−W4 (0.38 mol %) and TiO_2−Lut−W4 (0.19 mol %) because TiO_2−tBP contained the least amount of ligand on the TiO_2 surface initially. On the contrary, the TiO_2−Lut−W4 contains least amount of W4 because the largest amount of Lut ligand was already present on the TiO_2.

In addition, we also applied SCLC model to determine the electron mobility of three different TiO_2-pyridine derivative-W4. The mobility was further improved except TiO_2−Lut-W4, because it has the lowest amount of W4. On the contrary, the TiO_2-tBP-W4 exhibits the highest electron mobility (6.79×10^{-4} $cm^2/(V\ s)$) as compared to TiO_2−Pyridine-W4 (1.68×10^{-4} $cm^2/(V\ s)$) and TiO_2−Lut-W4 (8.95×10^{-5} $cm^2/(V\ s)$) (Figure 7a). To ensure the consistency between mobility measurement and device performance, we also applied the SCLC model on the above three P3HT: TiO_2-pyridine derivative-W4 hybrid thin film. The results are almost the same as TiO_2 only samples (Figure 7b), which indicate that W4 plays the vital role for efficient charge transfer in continuous TiO_2 percolation paths.

The power conversion efficiency of P3HT:TiO_2−tBP−W4 hybrid solar cell is about 1.36%, which is about 43 and 162% enhancement as compared to those of TiO_2−pyridine−W4 and TiO_2−Lut−W4 devices, respectively (Figure 8 and Table 3). The amount of enhancement is also in accordance with the amount of W4 molecules attached on TiO_2 surface. In P3HT:TiO_2−Lut−W4 devices, the suppression of W4 attachment is the main reason for its poor device performance, because, in the

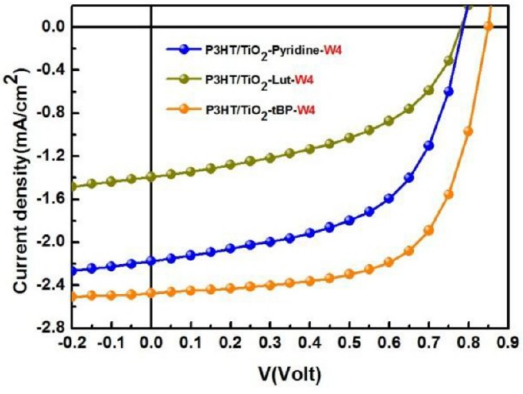

Figure 8. $J-V$ curves of different P3HT:TiO_2−(pyridine derivative)−W4 devices.

conversion process from light to electricity, the W4 molecule plays an important role to facilitate the charge separation and transport. In addition, the open-circuit voltage and short-circuit current of three devices using different W4 modified TiO_2 also followed the amount of W4 on TiO_2, it indicates that the higher dipole moment (8.64 debye) of conjugating W4 molecule has better band-tailing effect than nonconjugating molecules (pyridine derivatives). Furthermore, we also found that the anchoring of W4 molecules on TiO_2 nanorods could also improve its dispersion in P3HT domain as shown in the TEM photos of the P3HT: TiO_2–pyridine derivative–W4 hybrid films (Figure 9). Comparing to the island-shaped aggregation in

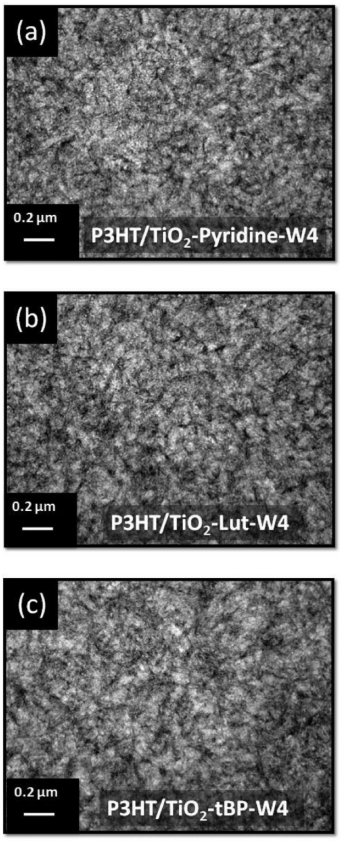

Figure 9. Transmission electron microscopy images of thin films by blending P3HT with (a) TiO_2–pyridine–W4, (b) TiO_2–Lut–W4, and (c) TiO_2–tBP–W4.

P3HT:TiO_2–tBP hybrid thin film (Figure 4d), the TiO_2–tBP–W4 can disperse well in P3HT domain and create a continuous transport path (Figure 9c) that results in enhanced power conversion efficiency.

CONCLUSION

In this work, we studied a two-stage surface modification with different surface modifiers for TiO_2 nanorods to enhance the performance of P3HT:TiO_2 hybrid solar cell. In the first-stage surface modification, three pyridine type ligands, pyridine, Lut, and tBP, with different pK_a values were used for TiO_2, respectively. The result of elemental analysis indicates the removing OA and attaching pyridine derivative occurred simultaneously in the ligand exchange process. In addition, the pKa value and surface tension of pyridine derivatives are the two most important factors which influence the removing and attaching reaction respectively. Subsequently, a small conjugating molecule (W4) was used in the second-stage of surface modification. The anchoring number of W4 on TiO_2 was determined by the amount of remaining pyridine derivative on TiO_2 after the first stage surface modification.

The electron mobility of TiO_2 increased with a decreasing amount of OA remaining after the first stage of modification. In addition, the electron mobility of TiO_2 was further enhanced by attaching conducting W4 after the second stage of surface modification. The aligned bandgap of W4 between P3HT and TiO_2 facilitates the charge separation and transport at interfaces. The TiO_2-tBP-W4 has the highest electron mobility due to the least amount of pyridine derivative and highest amount of W4 on TiO_2. Moreover, the hydrophobic W4 also helps the dispersion of TiO_2 in P3HT which results in the best performance solar cell among samples. The power conversion efficiency of P3HT:TiO_2–tBP–W4 device is about 1.36%, which is about 43 and 162% enhancement compared to TiO_2–pyridine–W4 and TiO_2–Lut–W4 devices, respectively.

In this investigation, we clearly demonstrate the effects of molecular structures of surface modifiers on the performance of P3HT:TiO_2 hybrid solar cells. The obtained knowledge can be extended to other hybrid solar cell system by properly design the surface modifier for colloid nanocrystals to achieve high power conversion efficiency.

EXPERIMENTAL SECTION

All chemicals were used as received. The anatase TiO_2 nanorods were synthesized by hydrolysis of titanium tetraisopropoxide (TTIP) according to literature.[26,27] First, oleic acid (OA, 180 g) was vigorously stirred for one hour in a three-neck flask under vacuum condition to remove any moisture. The solution was then heated to 98 °C and titanium tetraisopropoxide (25.5 mmol, Aldrich, 99.999%) was added into the flask and stirred for 10 minutes to mix well with the oleic acid. Trimethylamine-N-oxide dihydrate (51 mmol, Acros, 98%) in 25 ml of water was rapidly injected into the flask as a hydrolysis catalyst. This reaction was continued for 9 h to complete the hydrolysis and crystallization. Subsequently, the TiO_2–OA nanorods solution was obtained.

The as-synthesized TiO_2–OA nanorods were capped with insulating OA ligands. To remove the insulating OA molecules from TiO_2, the ligand exchange was carried out by two-stage surface modification. First, the TiO_2–OA nanorods (20 mL) were washed and precipitated by 20 ml methanol for four times to remove oleic acid molecules that were not tightly bound onto the surface of TiO_2 nanorods. Then, the pyridine type ligand (also called pyridine derivative for simplicity) (20 mL) was mixed with the TiO_2–OA nanorods by ultrasonic homogenizer (Branson model 2510). The mixture was then put into a three-neck flask and refluxed at 70 °C for 24 h under nitrogen flow to obtain a clear solution. In this step, oleic acid molecules could be replaced by pyridine derivatives and the modified TiO_2 nanorod was called as TiO_2–(pyridine derivative). Subsequently, in the second stage of surface modification, 3 mg conjugating surface modifiers, 2-cyano-3-(5-(7-(thiophen-2-yl)-benzothiadiazol-4-yl) thiophen-2-yl) acrylic acid (W4), was dissolved into this TiO_2–(pyridine derivative) solution. Then, the solution was also kept at 70°C and stirred for 24 h to allow the complete adsorption of W4 molecules onto the TiO_2 surface. We named the two-staged modified TiO_2 nanorods as TiO_2–(pyridine derivative)–W4 for simplicity. In the last, we used excess hexane to precipitate the two-staged modified TiO_2 nanorods and wash out the nonadsorbed W4 molecules.

In addition, the conducting polymer P3HT[28] and W4[29] were synthesized according to literature. The molecular weight of P3HT is 65 kDa, polydispersity (PDI) and regioregularity (RR) are 1.39 ± 0.06 and >95%, respectively.

The P3HT:TiO_2 hybrid solar cells were prepared by following procedure. First, the PEDOT:PSS solution (Baytron P VP AI 4083) was filtrated through 0.20μm PVDF filter and deposited on cleaned ITO glass (Luminescence Technology Corp., 10Ω) as hole transport layer. The PEDOT:PSS:ITO substrates were put in oven and dried at 120 °C for 40 min to remove the moisture. We then deposited a 30 nm P3HT buffer layer on PEDOT:PSS thin film to prevent the leakage current of devices. For preparing the P3HT:TiO_2 solution, we first dissolved P3HT by chlorobenzene with a concentration of 30 mg/mL, then the TiO_2 nanorods were redispersed in solvent mixture (pyridine:dicholoromethane:choloroform = 1:2:3) with a concentration of 12.5 mg/mL. The P3HT:TiO_2 nanorods hybrid solution with weight ratio of 47:53 was then spin-coated onto the P3HT:PEDOT:PSS thin film and the thickness was about 120 nm. To reduce the charge recombination at the interface between active layer and cathode, we spin-coated a 20 nm TiO_2 nanorods layer on the active layer as hole blocking layer. The sample was then stored in a glove box for 1 day for evaporating the residual solvent. After finishing the above steps, 100 nm of aluminum was thermally evaporated as cathode.

To clarify the effect of two-stage surface modification, we employed elemental analysis (Heraeus Virio El III, NCSH, Germany) to estimate the compositions of ligands on TiO_2 surface. The UV−visible absorption spectroscopy (PerkinElmer Lambda 35) was also used to monitor the adsorption behavior of W4 molecules after second-stage surface modification. For the sample preparation of TEM characterization, we spin-coated the P3HT:TiO_2 hybrid thin film on PEDOT/ITO substrate as mentioned above, and then immersed the sample into deionized water with tilting angle of 45°. After the immersion, the hybrid layer would float on the liquid surface, and we used copper mesh to collect the hybrid thin film and kept the sample in vacuum condition to remove water. Furthermore, we used the space limited charge current model to characterize charge mobility of different surface-modified TiO_2. In device characterization, the solar simulator (Newport, Model 66902) and voltage source meter (Keithley, Model 2410) were used for photovoltaic measurement.

■ ASSOCIATED CONTENT

Ⓢ Supporting Information

This material is available free of charge via the Internet at http://pubs.acs.org.

■ AUTHOR INFORMATION

Corresponding Author

*E-mail: suwf@ntu.edu.tw.

Notes

The authors declare no competing financial interest.

■ ACKNOWLEDGMENTS

Financial support obtained from the National Science Council of Taiwan (NSC 101-3113-E-002-010 and NSC 101-2120-M-002-003) is highly appreciated. We thank Dr. Chia-Hsin Wang, Dr. Yaw-Wen Yang, and Dr. Liang-Jen Fan of the National synchrotron radiation research center for the help in the characterization of X-ray photoelectron spectra.

■ REFERENCES

(1) Blouin, N.; Michaud, A.; Leclerc, M. *Adv. Mater.* **2007**, *19*, 2295−2300.
(2) Liang, Y. Y.; Wu, Y.; Feng, D. Q.; Tsai, S. T.; Son, H. J.; Li, G.; Yu, L. P. *J. Am. Chem. Soc.* **2009**, *131*, 56−57.
(3) Huo, L. J.; Hou, J. H.; Chen, H. Y.; Zhang, S. Q.; Jiang, Y.; Chen, T. L.; Yang, Y. *Macromolecules* **2009**, *42*, 6564−6571.
(4) Chen, H. Y.; Hou, J. H.; Zhang, S. Q.; Liang, Y. Y.; Yang, G. W.; Yang, Y.; Yu, L. P.; Wu, Y.; Li, G. *Nat. Photonics* **2009**, *3*, 649−653.
(5) Cheng, Y. J.; Hsieh, C. H.; He, Y. J.; Hsu, C. S.; Li, Y. F. *J. Am. Chem. Soc.* **2010**, *132*, 17381−17383.
(6) Khlyabich, P. P.; Burkhart, B.; Thompson, B. C. *J. Am. Chem. Soc.* **2011**, *133*, 14534−14537.
(7) Labram, J. G.; Kirkpatrick, J.; Bradley, D. D. C.; Anthopoulos, T. D. *Adv. Energy Mater.* **2011**, *1*, 1176−1183.
(8) Zhou, Y. F.; Eck, M.; Kruger, M. *Energy Environ. Sci.* **2010**, *3* (12), 1851−1864.
(9) Ren, S. Q.; Chang, L. Y.; Lim, S. K.; Zhao, J.; Smith, M.; Zhao, N.; Bulovic, V.; Bawendi, M.; Gradecak, S. *Nano Lett.* **2011**, *11* (9), 3998−4002.
(10) Noone, K. M.; Strein, E.; Anderson, N. C.; Wu, P. T.; Jenekhe, S. A.; Ginger, D. S. *Nano Lett.* **2010**, *10*, 2635−2639.
(11) Chen, H. C.; Lai, C. W.; Wu, I. C.; Pan, H. R.; Chen, I. W. P.; Peng, Y. K.; Liu, C. L.; Chen, C. H.; Chou, P. T. *Adv. Mater.* **2011**, *23*, 5451−5455.
(12) Zhang, Q. L.; Russell, T. P.; Emrick, T. *Chem Mater* **2007**, *19*, 3712−3716.
(13) Dayal, S.; Kopidakis, N.; Olson, D. C.; Ginley, D. S.; Rumbles, G. *Nano Lett* **2010**, *10*, 239−242.
(14) Lokteva, I.; Radychev, N.; Witt, F.; Borchert, H.; Parisi, J.; Kolny-Olesiak, J. *J. Phys. Chem. C* **2010**, *114* (29), 12784−12791.
(15) Monson, T. C.; Lloyd, M. T.; Olson, D. C.; Lee, Y. J.; Hsu, J. W. P. *Adv. Mater.* **2008**, *20* (24), 4755−4759.
(16) Lloyd, M. T.; Prasankumar, R. P.; Sinclair, M. B.; Mayer, A. C.; Olson, D. C.; Hsu, J. W. P. *J. Mater. Chem.* **2009**, *19*, 4609−4614.
(17) Shao, S. Y.; Liu, F. M.; Fang, G.; Zhang, B. H.; Xie, Z. Y.; Wang, L. X. *Org. Electron.* **2011**, *12*, 641−647.
(18) Said, A. J.; Poize, G.; Martini, C.; Ferry, D.; Marine, W.; Giorgio, S.; Fages, F.; Hocq, J.; Boucle, J.; Nelson, J.; Durrant, J. R.; Ackermann, J. *J. Phys. Chem. C* **2010**, *114*, 11273−11278.
(19) Ravirajan, P.; Peiro, A. M.; Nazeeruddin, M. K.; Graetzel, M.; Bradley, D. D. C.; Durrant, J. R.; Nelson, J. *J. Phys. Chem. B* **2006**, *110*, 7635−7639.
(20) Lin, Y. Y.; Chu, T. H.; Chen, C. W.; Su, W. F. *Appl. Phys. Lett.* **2008**, *92*, 053312.
(21) Huang, Y. C.; Yen, W. C.; Liao, Y. C.; Yu, Y. C.; Hsu, C. C.; Ho, M. L.; Chou, P. T.; Su, W. F. *Appl. Phys. Lett.* **2010**, *96*, 123501.
(22) Lin, Y. Y.; Chu, T. H.; Li, S. S.; Chuang, C. H.; Chang, C. H.; Su, W. F.; Chang, C. P.; Chu, M. W.; Chen, C. W. *J. Am. Chem. Soc.* **2009**, *131*, 3644−3649.
(23) Huang, Y. C.; Hsu, J. H.; Liao, Y. C.; Yen, W. C.; Li, S. S.; Lin, S. T.; Chen, C. W.; Su, W. F. *J. Mater. Chem.* **2011**, *21*, 4450−4456.
(24) Huang, Y. C.; Chuang, S. Y.; Wu, M. C.; Chen, H. L.; Chen, C. W.; Su, W. F. *J. Appl. Phys.* **2009**, *106*, 034506.
(25) Liao, H. C.; Lee, C. H.; Ho, Y. C.; Jao, M. H.; Tsai, C. M.; Chuang, C. M.; Shyue, J. J.; Chen, Y. F.; Su, W. F. *J. Mater. Chem.* **2012**, *22*, 10589−10596.
(26) Lin, Y. T.; Zeng, T. W.; Lai, W. Z.; Chen, C. W.; Lin, Y. Y.; Chang, Y. S.; Su, W. F. *Nanotechnology* **2006**, *17*, 5781−5785.
(27) Zeng, T. W.; Lin, Y. Y.; Lo, H. H.; Chen, C. W.; Chen, C. H.; Liou, S. C.; Huang, H. Y.; Su, W. F. *Nanotechnology* **2006**, *17*, 5387−5392.
(28) Ho, C.C.; Liu, Y.C.; Lin, S.H.; Su, W. F. *Macromolecules* **2012**, *45*, 813−820.
(29) Yu, J.; Shen, T. L.; Weng, W. H.; Huang, Y. C.; Huang, C. I.; Su, W. F.; Rwei, S. P.; Ho, K. C.; Wang, L. *Adv. Energy Mater.* **2012**, *2*, 245−252.
(30) Cozzoli, P. D.; Kornowski, A.; Weller, H. *J. Am. Chem. Soc.* **2003**, *125*, 14539−14548.
(31) Morandeira, A.; Lopez-Duarte, I.; O'Regan, B.; Martinez-Diaz, M. V.; Forneli, A.; Palomares, E.; Torres, T.; Durrant, J. R. *J. Mater. Chem.* **2009**, *19*, 5016−5026.
(32) Nazeeruddin, M. K.; Kay, A.; Rodicio, I.; Humphrybaker, R.; Muller, E.; Liska, P.; Vlachopoulos, N.; Gratzel, M. *J. Am. Chem. Soc.* **1993**, *115*, 6382−6390.
(33) Zhu, R.; Jiang, C. Y.; Liu, B.; Ramakrishna, S. *Adv. Mater.* **2009**, *21*, 994−1000.
(34) Yu, S.; Ahmadi, S.; Sun, C. H.; Palmgren, P.; Hennies, F.; Zuleta, M.; Gothelid, M. *J. Phys. Chem. C* **2010**, *114*, 2315−2320.

(35) Kusama, H.; Orita, H.; Sugihara, H. *Sol. Energy Mater. Sol. Cells* **2008**, *92*, 84−87.
(36) Gothelid, M.; Yu, S.; Ahmadi, S.; Sun, C. H.; Zuleta, M. *Int. J. Photoenergy* **2011**, 401356.
(37) Durr, M.; Yasuda, A.; Nelles, G. *Appl. Phys. Lett.* **2006**, *89*, 061110.
(38) Goh, C.; Scully, S. R.; McGehee, M. D. *J. Appl. Phys.* **2007**, *101*, 114503.
(39) Liu, Y. X.; Scully, S. R.; McGehee, M. D.; Liu, J. S.; Luscombe, C. K.; Frechet, J. M. J.; Shaheen, S. E.; Ginley, D. S. *J. Phys. Chem. B* **2006**, *110*, 3257−3261.
(40) Monte, M. B. M.; Coelho, R. R.; Middea, A. *Petrol. Sci. Technol.* **2004**, *22* (7−8), 991−1001.
(41) Mihm, L. D. A.; Coutinho, L. F.; Meirelles, A. J. A. *J. Am. Oil Chem. Soc.* **1999**, *76*, 379−382.
(42) Brown, H. C.; Mihm, X. R. *J. Am. Chem. Soc.* **1955**, *77*, 1723−1726.